

## Original Article

# Biomechanical effects of different lateral mass injury patterns on subaxial cervical fracture dislocations after anterior cervical surgery: a finite element study

Junsong Yang\*, Qingda Li\*, Peng Liu, Liang Yan\*, Tuanjiang Liu, Jijun Liu\*, Qinpeng Zhao, Baorong He, He Zhao, Bing Qian, Yuanting Zhao\*, Dingjun Hao

*Department of Spine Surgery, Honghui Hospital, Xi'an Jiaotong University, No. 76, Nanguo Road, Beilin District, Xi'an 710054, Shaanxi, China. \*Equal contributors.*

Received May 15, 2021; Accepted March 30, 2022; Epub September 15, 2022; Published September 30, 2022

**Abstract:** Objective: The lateral mass joint plays an important role in maintaining the mechanical stability of the subaxial cervical spine. We first performed a three-dimensional finite element (FE) biomechanical study to evaluate the local mechanical stability of subaxial cervical fracture dislocations after anterior-only fixation for lateral mass injuries of varying severity. Methods: A three-dimensional FE model of the subaxial cervical spine with simple anterior fixation for C5-6 fracture dislocation was reconstructed. According to their different morphological characteristics of unilateral lateral mass injuries, the lateral mass injury was divided into six types. The range of motion (ROM) of each part and the stress of the cage, each intervertebral disc, titanium plate, and screw stress were recorded. Results: The ROM of C3-4, C4-5, C5-6, and C6-7 in type 4 was higher than that of the other five types. The maximum equivalent stress on C4-5 intervertebral discs, titanium plates, and screws in type 4 under various sports loads was higher than that produced by the other load types. In the stress cloud diagram of the front titanium plate and screws, the degree of stress was the highest in type 4. Stress placed on each part of the model, from high to low, was as follows: plate, screw, C6, C5, and C7. Conclusion: Greater injury severity is associated with higher stress on the plate and screw with exercise loads. Type 4 lateral mass injuries, characterized by ipsilateral pedicle and lamina junction fractures, significantly affected biomechanical stability after simple anterior fixation.

**Keywords:** Subaxial cervical spine injury, anterior plate, biomechanics, finite element analysis

## Introduction

Subaxial cervical injuries (SCI) refer to C3-7 segment injuries, which account for approximately 65% of all cervical spine injuries [1]. Two-thirds of cervical fractures and three-quarters of cervical dislocations are located between C5 and C7 [2]. As mechanisms of injury vary greatly, there are diverse forms of SCI. AOSpine (2016) divides SCI into three types: A, B, and C [3]. There is no dispute regarding the treatment of type A and B SCI. Type C SCI include subaxial cervical fracture dislocations (SCFDs), which account for approximately 7% of cervical spine trauma, with about 87% of patients displaying varying degrees of neurological deficits [4, 5]. The incidence of traumatic disc herniation (TDH) is high because SCFDs are often accompanied by unilateral or bilateral

facet joint strangulation, and the optimal surgical approach for treating these injuries remains controversial [6, 7].

The combined anterior and posterior surgical approach is regarded as a stable and reliable treatment option, and simultaneous decompression of the ventral and dorsal spinal cord is achievable, but the associated trauma is significant. The recovery rate is slow, and the cost of treatment is high [8]. Utilization of the posterior approach alone reduces vertebral dislocation and can promote the recovery of neurological function. However, the posterior approach requires extensive dissection of the neck muscles, resulting in greater blood loss and incidence of postoperative infection and axial pain compared with the anterior approach [9-11]. Surgery via the anterior approach is associated

## Biomechanical study of LM injury in SCFDs

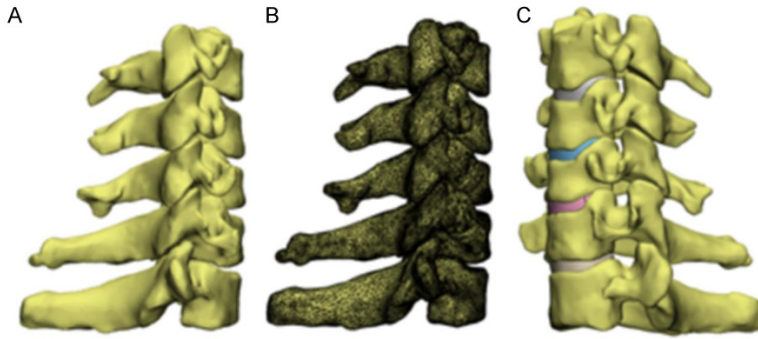


**Figure 1.** C3-7 normal subaxial cervical spine solid model. A. The geometric model. B. The remesh model. C. The assembled model with intervertebral disc model.

with less trauma, and ideal decompression of the ventral spinal cord is achievable in the treatment of TDH [12]. However, some patients experience postoperative internal fixation loosening or even delayed cervical kyphosis [13-15]. This leads to the need for a second revision surgery, greatly increasing the economic burden on patients. Therefore, it is necessary to quantitatively evaluate the degree of injury of subaxial cervical spine fractures and dislocations and identify patients who are prone to internal fixation failure after simple anterior fixation.

The lateral mass joint plays an important role in maintaining the mechanical stability of the subaxial cervical spine. Therefore, the latest AOSpine subaxial cervical spine classification considers the lateral mass joint as an independent dimension for the classification of SCI [3]. They are divided into four types in increasing order of severity: F1-F4. In addition to this classification, we also found that a lateral mass split fracture is a common form of lateral mass injury. To determine whether different lateral mass damage patterns affect local mechanical stability at the subaxial cervical spine after simple anterior fixation, we intended to evaluate local mechanical stability after simple anterior fixation through three-dimensional finite element (FE) modeling and analysis.

### Materials and methods

#### Research participants

The study was approved by the medical ethics committee of the Honghui Hospital, Xi'an Jiaotong University (No. 202102007), in accordance with the relevant guidelines and regula-

tions. A healthy man aged 32 years (height, 175 cm; weight, 70 kg) voluntarily participated in the study, with informed consent. He had no history of cervical spine trauma or surgery, occipital cervical spine degeneration, tumors, deformities, or infections. Using 256-slice spiral computed tomography (CT) (Siemens Light Speed; Germany), the volunteer was scanned (120 kV, 125 mA, scan thickness 0.75 mm, range C3-7). CT data were exported

and saved in the digital imaging and communications in medicine (DICOM) format, and a total of 413 images were obtained.

#### Development of FE C3-7 spine model

CT scan data were imported into Mimics software (20.0) (Materialize, Belgium), which was used to read image data, segment tissue, repair processing geometry, select the human bone threshold, establish the C3-7 normal subaxial cervical spine geometry model, and save data in a binary STereoLithography (STL) format file. The STL file was imported into Mimics' own digital forward engineering 3-matic 12.0 software for repairing, smoothing, and designing intervertebral discs, ligaments, and so on (Figure 1).

A computer-aided design (CAD) software (CREO 3.0) was used to design anterior cervical titanium plates, screws, and intervertebral fusion cages. The anterior cervical plate refers to the American Johnson skyline anterior cervical fixation system. The length of the titanium plate is 25 mm, and its width is 16 mm, thickness is 2.5 mm, outer diameter is 4.0 mm, and length of the titanium screws is 14 mm. The American Medtronic's Cornerstone intervertebral fusion cage has a length of 25 mm, width of 16 mm, and height of 2.5 mm. Each model was imported into Geomagic 13.0 (Geomagic Company, USA), and an accurate curve module was used for surface construction, repair, sanding, denoising, cutting, smoothing, and other processing of the model. The same software was used to initially synthesize the C3-7 normal subaxial cervical spine solid model. In the C5-6 segment, the intervertebral disc was removed, an intervertebral fusion cage was inserted, and the anterior cervical plate screw was fixed in

## Biomechanical study of LM injury in SCFDs

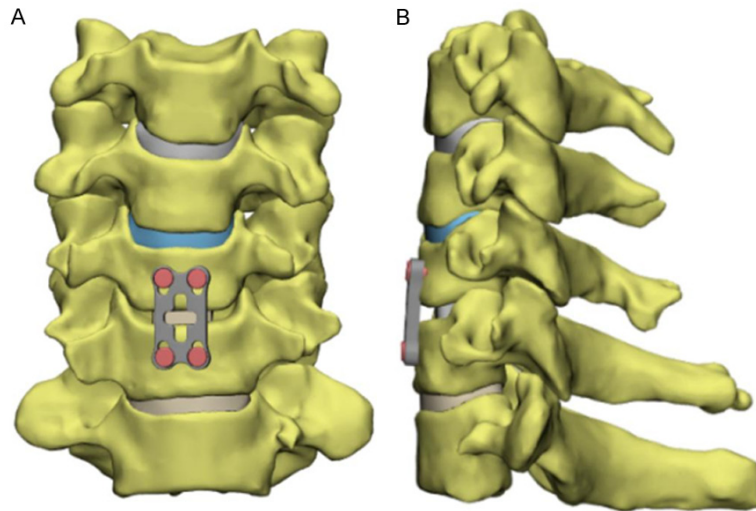


**Figure 2.** C3-7 normal subaxial cervical spine solid model. In the C5-6 segment, the intervertebral disc was removed, an intervertebral fusion cage was inserted, and the anterior cervical plate screw was fixed in front of C5-6. A. Anteroposterior view. B. Lateral view.

**Table 1.** Element and node number of the finite element model

	Elements	Nodes
C3 cortical bone + cancellous bone	56989	100471
C3-C4 intervertebral disc	6593	12093
C4 cortical bone + cancellous bone	45436	80711
C4-C5 intervertebral disc	7288	13218
C5 cortical bone + cancellous bone	109300	189770
Cage	5248	9391
C6 cortical bone + cancellous bone	116749	204970
C6-C7 intervertebral disc	8585	15639
C7 cortical bone + cancellous bone	67961	123131
Titanium plate	42032	74606
Screw	61319	107888
Ligament	631	1109
Total	526869	932997

**Table 2.** Element types and material properties of the finite element model of the subaxial cervical spine

Material	Density (kg/m <sup>3</sup> )	Young's modulus (GPa)	Poisson's ratio
Ti6Al4V	4500	110	0.31
Cortical bone	-	12	0.3
Cancellous bone	-	0.1	0.2
Intervertebral disc	-	0.5	0.45
Cage	-	3.6	0.44

front of C5-6 (**Figure 2**). Finally, all models were imported into a general FE software, ANSYS

Workbench 20.0 (Ansys, USA), to assemble in the Design Modeler (DM) module, and the C3-7 normal subaxial cervical spine three-dimensional FE model was established.

### *Dividing the network*

The meshing command was used to mesh lines of each model, refine the endplate of the key analysis, and add grid data (**Table 1**).

### *Defining material properties*

The materials used when creating this model included titanium alloy (Ti6Al4V), cortical bone, cancellous bone, intervertebral discs, and an interbody fusion cage. Cervical vertebrae, posterior structure, intervertebral disc annulus fibrosus, and nucleus pulposus were simulated as tetrahedral units (**Table 2**).

### *Defining ligaments and contact types*

A nonlinear cable element was used to simulate characteristics of a ligament, which was under tension only, and not compression. Simulated ligaments included the anterior longitudinal, posterior longitudinal, articular capsule, ligamentum flavum, interspinous, and supraspinous ligaments. A total of eight bilateral contralateral mass joints of C3-7 were defined with face-to-face contact. Because the joint was encased in the joint capsule, friction between the joint surfaces was very small due to the presence of the synovium and synovial fluid. Therefore, the face-to-face contacts between joints of the model were defined as having non-friction characteristics (**Table 3**).

### *Setting boundary conditions and loads*

Using the three-dimensional FE ANSYS 20.0 (ANSYS Company, USA) analysis software, six

**Table 3.** Ligament material properties of the subaxial cervical spine finite element model

Style	Elastic modulus (Mpa)	Poisson's ratio	Cross sectional area (mm <sup>2</sup> )
Anterior longitudinal ligament	30	0.3	6.1
Posterior longitudinal ligament	20	0.3	5.4
Ligament of articular capsule	20	0.3	46.6
Ligamentum flavum	10	0.3	50.1
Interspinous ligament	1.5	0.3	13.1
Supraspinous ligament	28	0.3	28

degrees of freedom of the C7 vertebral body bottom of all the scheme models were fully constrained and fixed. At the same time, the pure torque of 1.5 N × m of flexion, extension, left flexion, and left rotation (**Figure 3**) was applied to the C3 vertebral body to perform flexion, extension, lateral flexion, and rotation of the cervical spine.

*Verification of FE model*

Using settings described in classic in vitro biomechanics experiments by Panjabi [16] and Ng [17], six degrees of freedom of the lower edge of the C7 in the three-dimensional FE model of the cervical spine were constrained. Then, 50 N was applied to the occipital bone (simulating cranial weight), and a torque of 1.5 N × m was applied according to the conditions of flexion, extension, lateral bending, and rotation. Flexion and extension movements occurred along the coronal plane, the lateral bending movement occurred along the sagittal plane, and axial rotation produced movement in a direction tangent to the cervical spine.

*Experimental grouping*

According to the different morphological characteristics of unilateral lateral mass injuries, the lateral mass injury can be divided into six types (**Figure 4**). Type 1 is characterized by complete split fracture of the lateral mass. Type 2 is characterized by partial split fracture of the lateral mass. Type 3 is characterized by severe avulsion fracture of the lateral mass. Type 4 is characterized by simultaneous disconnection of the pedicle, lateral mass, and ipsilateral lamina. Type 5 is characterized by mild avulsion fracture of the lateral mass. As the control group, type 6 is characterized by an intact lateral mass without bony injury.

*Model validation*

The three-dimensional FE model of the C3-7 subaxial cervical spine consisted of 526,869 elements and 932,997 nodes. In terms of geometry and morphology, the appearance of the model fit reality, and its fidelity and precision were ideal. Through a comparison with the results of Panjabi [16]

and Ng [17], the results of classical in vitro subaxial cervical biomechanical tests revealed that the complete subaxial cervical spine model established in this study was able to effectively simulate activities of cervical flexion and extension, lateral flexion, and rotation in all directions, and the range of motion (ROM) of a single segment in flexion and extension, lateral flexion, and axial rotation (**Figure 5**) was consistent with the reference. Only a small part of the results is consistent with the reference, and there was an offset within 2° of the range. Therefore, the subaxial cervical spine model constructed in this study was validated. The ROM of each part and the stress of cage, each intervertebral disc, titanium plate, and screw stress were recorded.

**Results**

*ROM*

According to the overall size of the C3-4, C4-5, C5-6, and C6-7 spine models and the maximum deformation under the state of exercise load, activities of the spine in flexion, extension, left flexion, and left rotation were calculated (**Figure 6**). The ROM of C3-4, C4-5, C5-6, and C6-7 in type 4 was higher than that in the other five types. At the C3-4 segment, the ROM of anterior flexion (AF) was 40.71°, retroextension (RE) was 26.25°, left flexion (LF) was 25.97°, and left rotation (LR) was 16.49°. Regarding the C4-5 segment, the ROM of AF was 25.36°, RE was 19.23°, LF was 21.86°, and LR was 16.89. For the C6-7 segment, the ROM for AF was 15.56°, RE was 13.84°, LF was 13.54°, and LR was 12.51°. The ROM of the C5-6 segment was the lowest in all four segments. The ROM for AF was 3.79°, RE was 1.01°, LF was 5.34°, and LR was 4.66°.

## Biomechanical study of LM injury in SCFDs

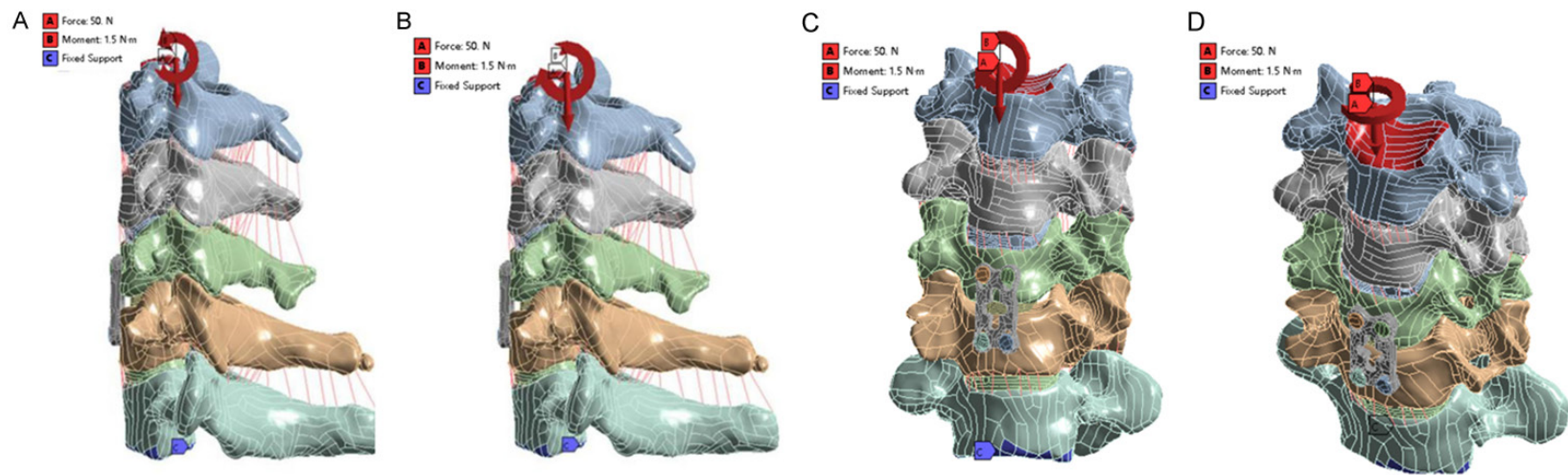


**Figure 3.** C3-7 normal subaxial cervical spine solid model under the pure torque of  $1.5 \text{ N} \times \text{m}$  of flexion (A), extension (B), left flexion (C), and left rotation (D).

## Biomechanical study of LM injury in SCFDs

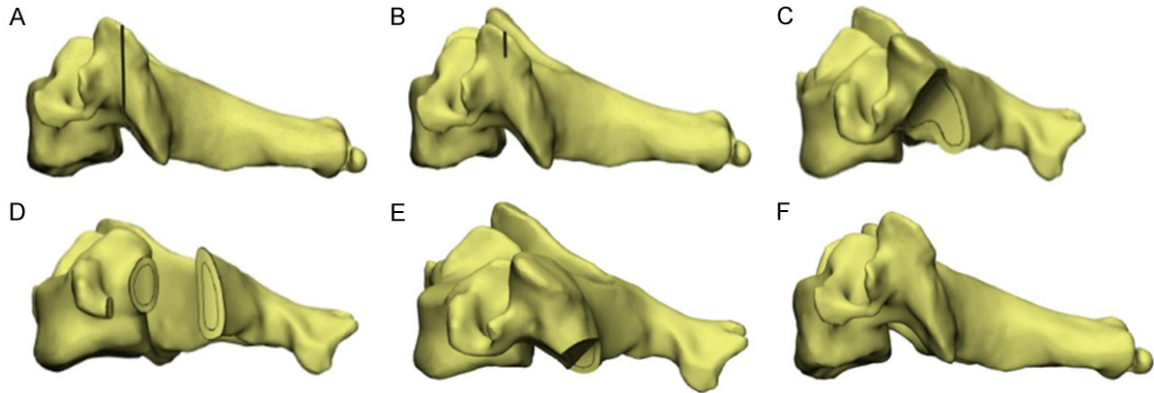


**Figure 4.** Six types of lateral mass injuries. Type 1 is characterized by complete split fracture of the lateral mass (A). Type 2 is characterized by partial split fracture of the lateral mass (B). Type 3 is characterized by severe avulsion fracture of the lateral mass (C). Type 4 is characterized by simultaneous disconnection of the pedicle, lateral mass, and ipsilateral lamina (D). Type 5 is characterized by mild avulsion fracture of the lateral mass (E). As the control group, type 6 is characterized by intact lateral mass without bony injury (F).

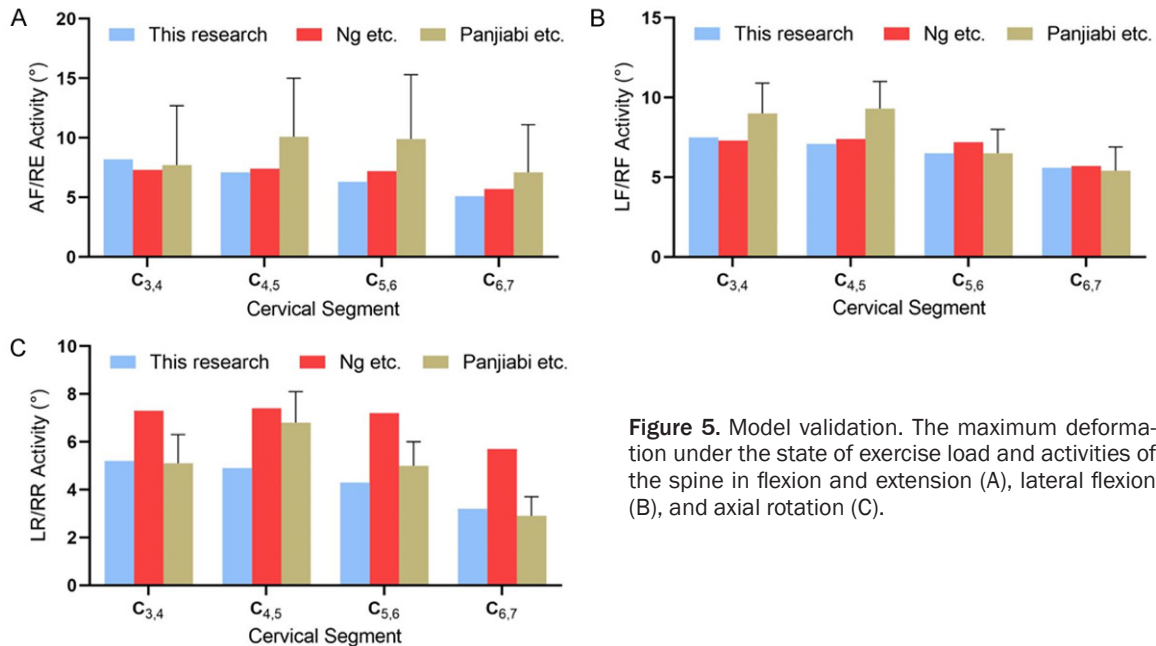


**Figure 5.** Model validation. The maximum deformation under the state of exercise load and activities of the spine in flexion and extension (A), lateral flexion (B), and axial rotation (C).

### Cage, intervertebral disc, titanium plate, and screw stress

The maximum equivalent stress of the C3-4 intervertebral disc, C4-5 intervertebral disc, C5-6 intervertebral fusion cage, C6-7 intervertebral disc, titanium plate, and screws in the four states of AF, RE, LF, and LR of the six types were calculated (**Figure 7**). The maximal von mises stress at the C4-5 intervertebral discs and the cage of the C5-6 space was slightly higher than that at the C3-4 and C6-7 inter-

tebral discs in all six types. Since the stress after fusion is more concentrated in the upper segment, the stress of C4-5 is greater than that of C5-6. The maximal von mises stress on the titanium plates and screws in type 4 under various sports loads is higher than that produced by the other five load types, especially at the position of AF. A stress cloud diagram of the front titanium plate and screws is shown in **Figures 8-13**. Stress to the plate and screw was mainly concentrated in and around the screw-plate interface.

## Biomechanical study of LM injury in SCFDs

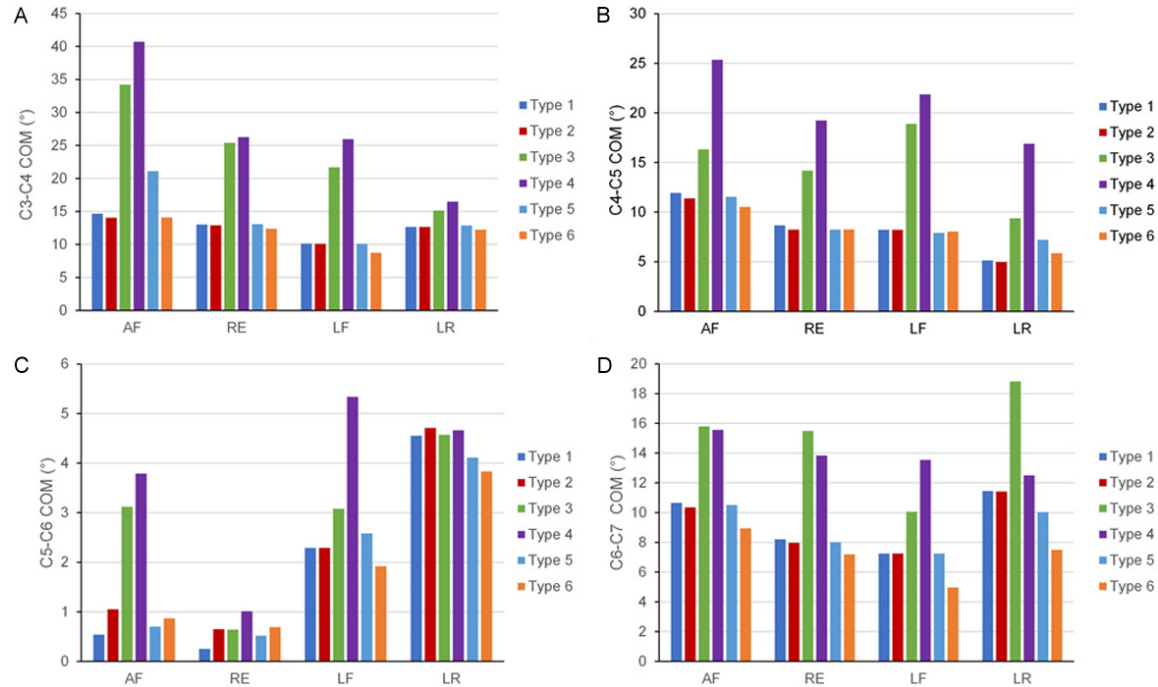


**Figure 6.** The maximum deformation under the state of exercise load, activities of the spine in flexion, extension, left flexion, and left rotation, including C3-4 (A), C4-5 (B), C5-6 (C), and C6-7 (D).

### Discussion

#### *FE analysis characteristics and model validity*

Biomechanical research plays an important role in the pathogenesis and evaluation of surgical efficacy. In the past, mechanical analyses of cervical vertebrae mainly required cervical corpses of humans or primates or other mammals. This method mainly involves the measurement of anatomy using a simple motion model of components, which has great scope of application and the basic data is conveniently accessible. It is especially suitable for studying anatomical factors that function as principle influencing parameters, such as overall and local biomechanical performance and mobility of the cervical spine internal fixation device complex after implantation of the cervical internal fixation device. Panjabi et al. [16, 18] established a standard for creating a three-dimensional motion model of upper cervical segments of human corpses. They quantitatively measured changes in muscles, ligaments, and spinal nerves after cervical whiplash injury, which provided an important reference for subsequent clinical diagnoses and treatments. However, the above-mentioned cadaveric tests have some limitations, such as difficulty in

obtaining cadaveric specimens, low repeatability, and difficulty with regard to quantifying changes in internal stress of the vertebral body, intervertebral disc, lateral mass joint, joint capsule, and posterior ligament.

Three-dimensional FE analysis may be performed while different loads, material properties, boundary conditions, stresses, strain types, degrees of stiffness, and types of displacement are applied in the model; this is helpful for clarifying complex biomechanical characteristics of the spine and has improved repeatability, reduced cost, and saved time. A three-dimensional FE model of the subaxial cervical spine was established based on CT scanning data and a series of software programs, which included 526,869 elements and 932,997 nodes. The ROM of the cervical spine was determined to be similar to that determined by Panjabi [16] and Ng [17], but differences between the data of our model and theirs were observed in some segments. Due to differences between studies on the ROM of three-dimensional FE models, we consider effects of many confounding factors such as race, age, degree of cervical degeneration, and various material property parameter settings, as well as the influence of the modeling opera-

## Biomechanical study of LM injury in SCFDs

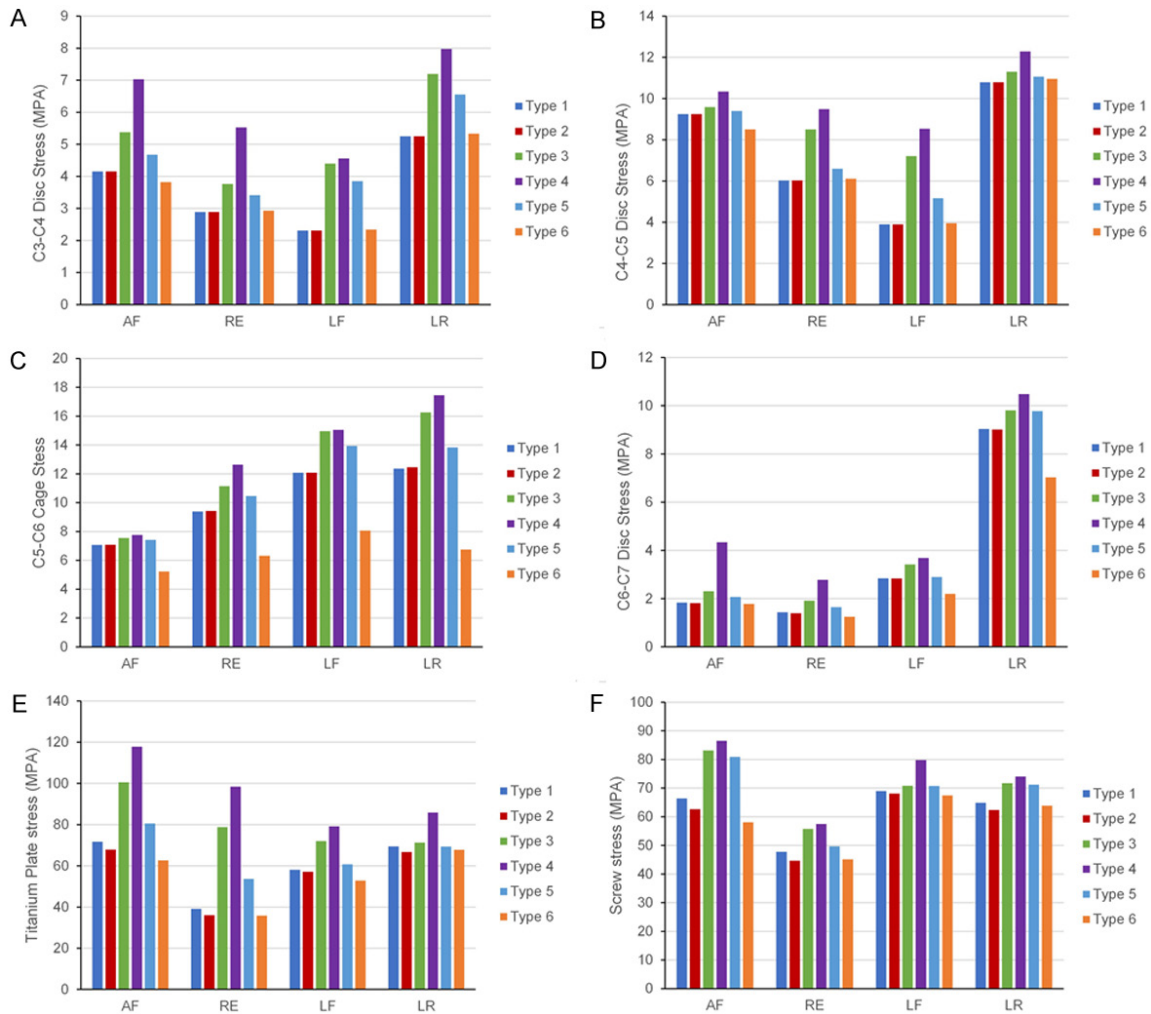


**Figure 7.** The maximum equivalent stress of the C3-4 intervertebral disc (A), C4-5 intervertebral disc (B), C5-6 intervertebral fusion cage (C), C6-7 intervertebral disc (D), titanium plate (E), and screws (F) in the four states of flexion, extension, left flexion, and left rotation of the six types of lateral mass injuries.

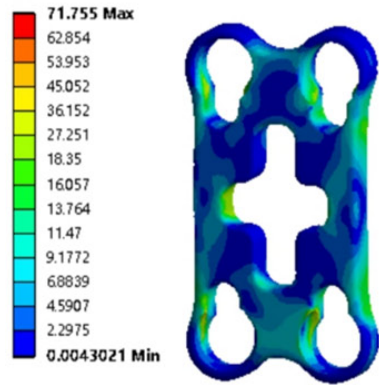
tion itself on the accuracy of the model, which may lead to some heterogeneity between different models. In conclusion, the subaxial cervical spine model constructed in this study can simulate biomechanical tests of the cervical spine through validation.

### ROM of each segment

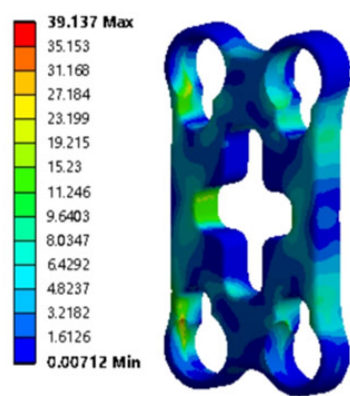
As C5-6 is fixed by plate and screws, the segmental ROM is lower than that of other segments. The ROM of C3-4, C4-5, C5-6, and C6-7 was higher than that of the other five types. Previous biomechanical studies also showed that the intervertebral disc mobility of adjacent segments increases more significantly after C5-6 segment fusion versus under physiological conditions [19, 20]. This may be because

SCFDs are often accompanied by lateral mass fractures and posterior ligament complex (PLC) injuries. Due to differing in injury mechanisms and the severity of high-energy violence, the fracture morphology of the lateral mass and degree of PLC injury differ. Therefore, we suspect that the occurrence of different lateral fast injury morphologies may be important in internal fixation failure after repair via the anterior approach. Our study found that different injury patterns affect the rigidity of anterior fixation and increase the ROM of the remaining discs. Further analysis of different injury patterns showed that complete lateral mass detachment (type 4) had the greatest influence on ROM, and the stability of lateral mass avulsion fracture was compared with that of split fracture. The subgroup analysis showed that there

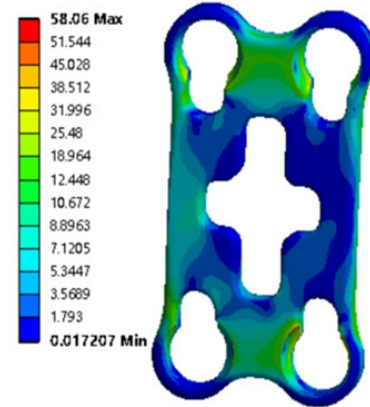
### Flexion



### Extension



### Left flexion



### Left rotation

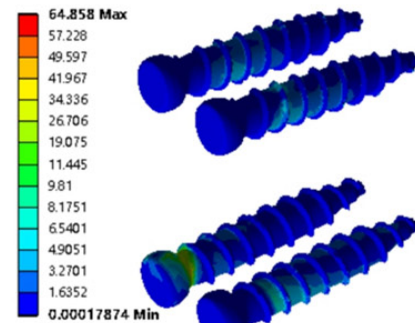
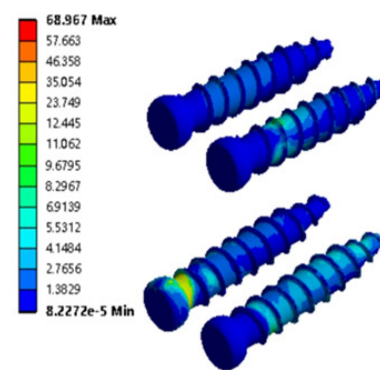
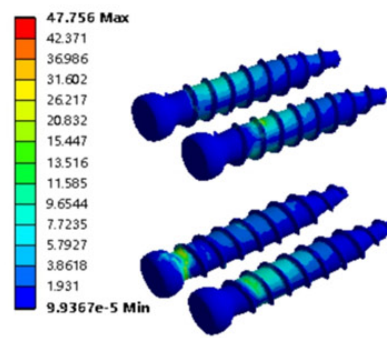
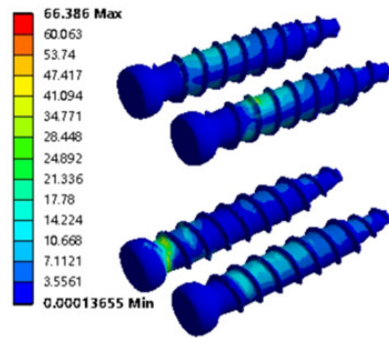
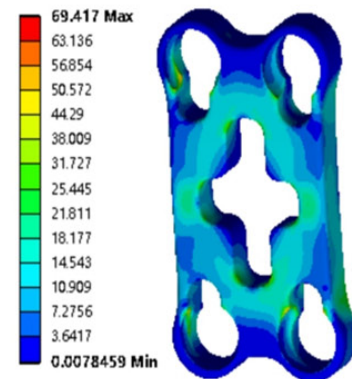


Figure 8. The stress cloud diagram of the front titanium plate and screws of the type 1 of lateral mass injury.

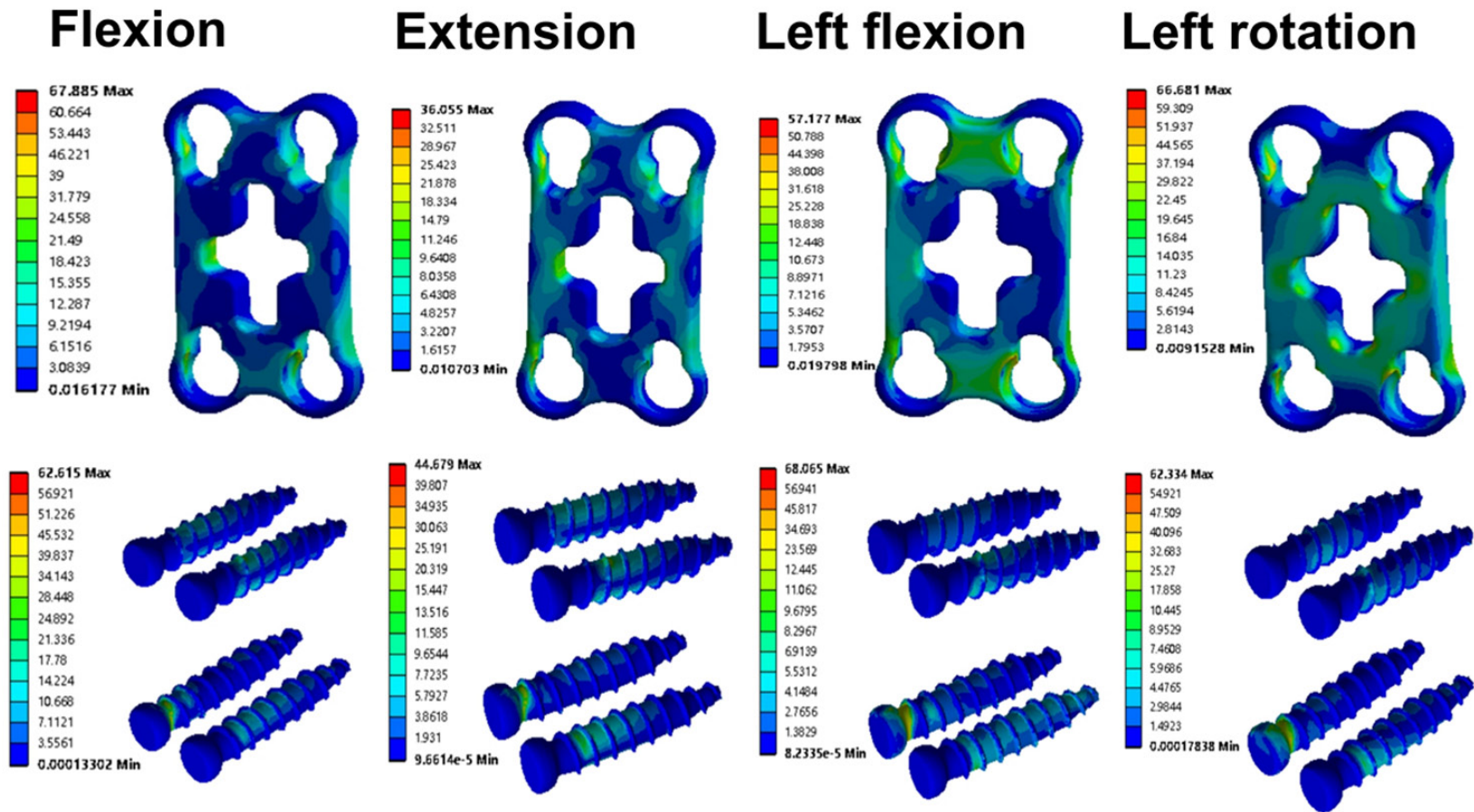


Figure 9. The stress cloud diagram of the front titanium plate and screws of the type 2 of lateral mass injury.

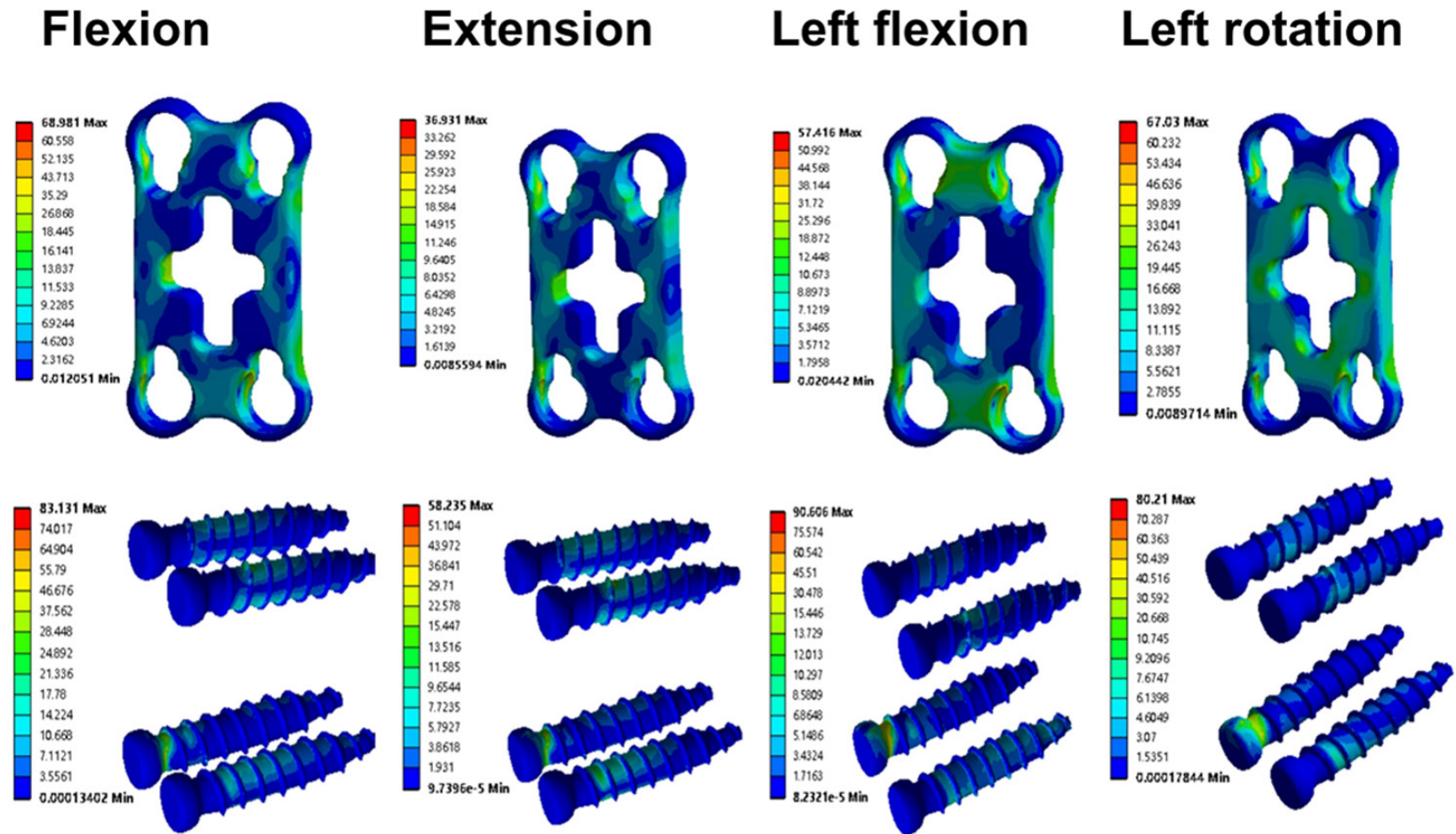


Figure 10. The stress cloud diagram of the front titanium plate and screws of the type 3 of lateral mass injury.

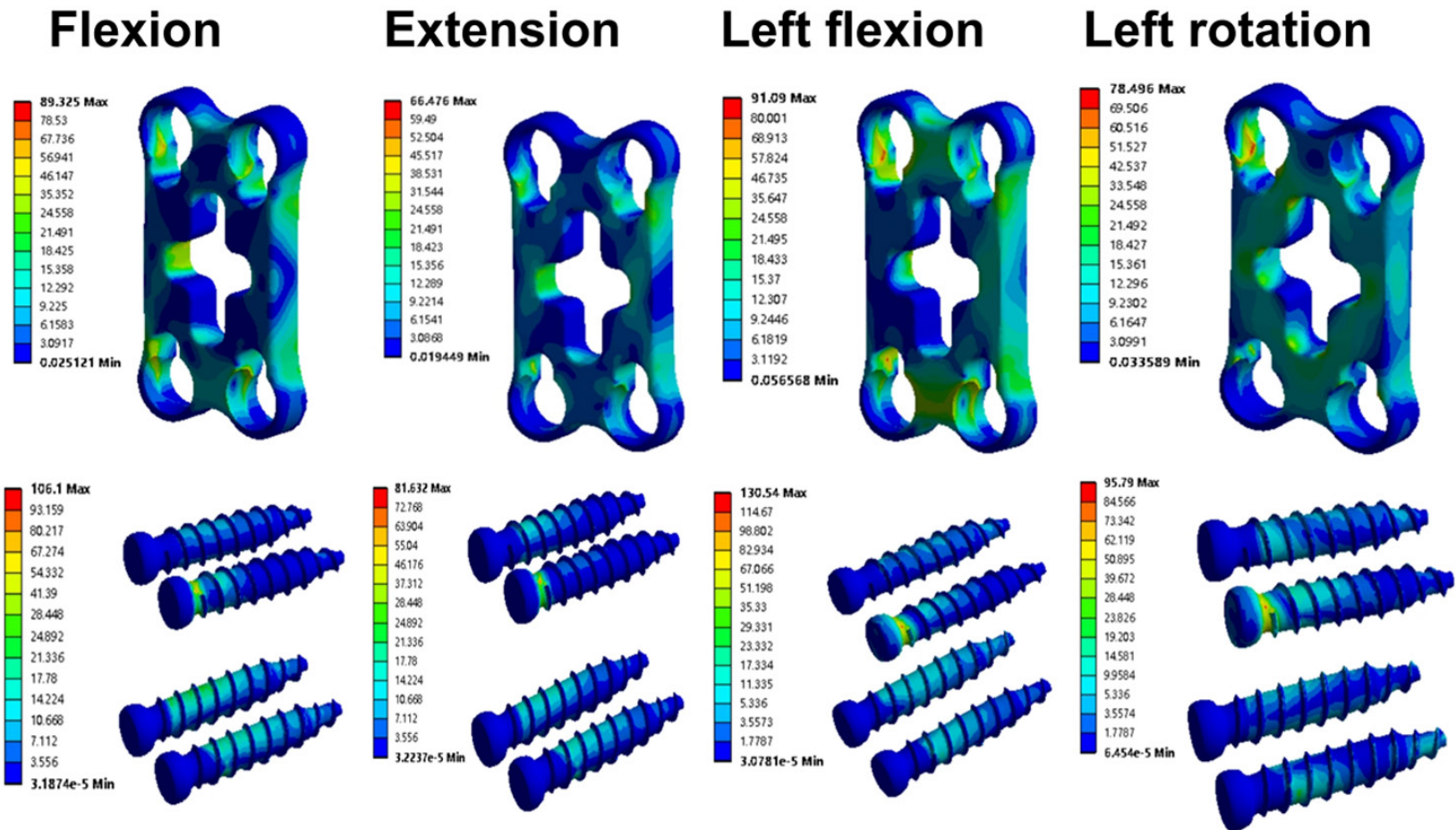


Figure 11. The stress cloud diagram of the front titanium plate and screws of the type 4 of lateral mass injury.

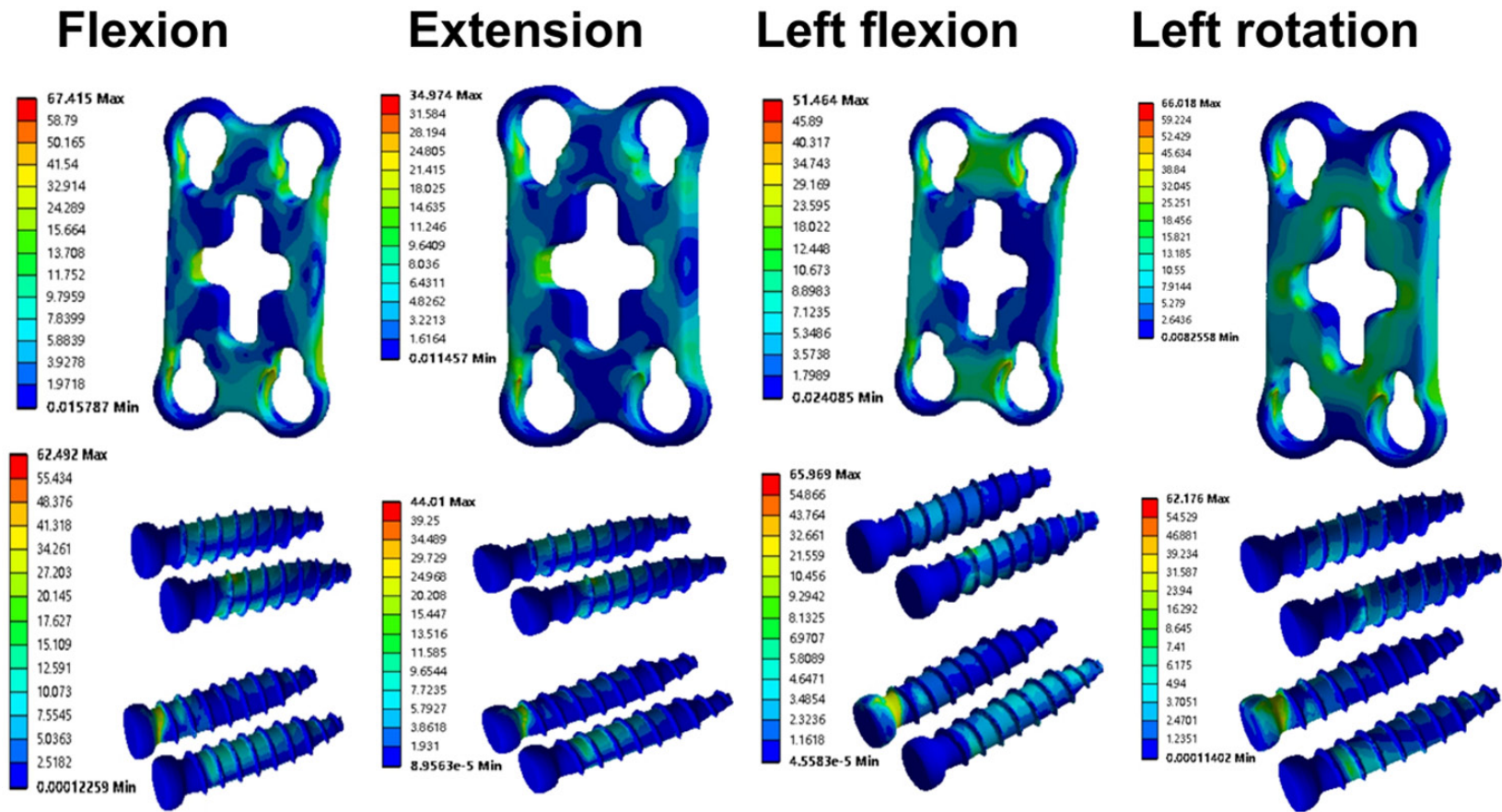


Figure 12. The stress cloud diagram of the front titanium plate and screws of the type 5 of lateral mass injury.

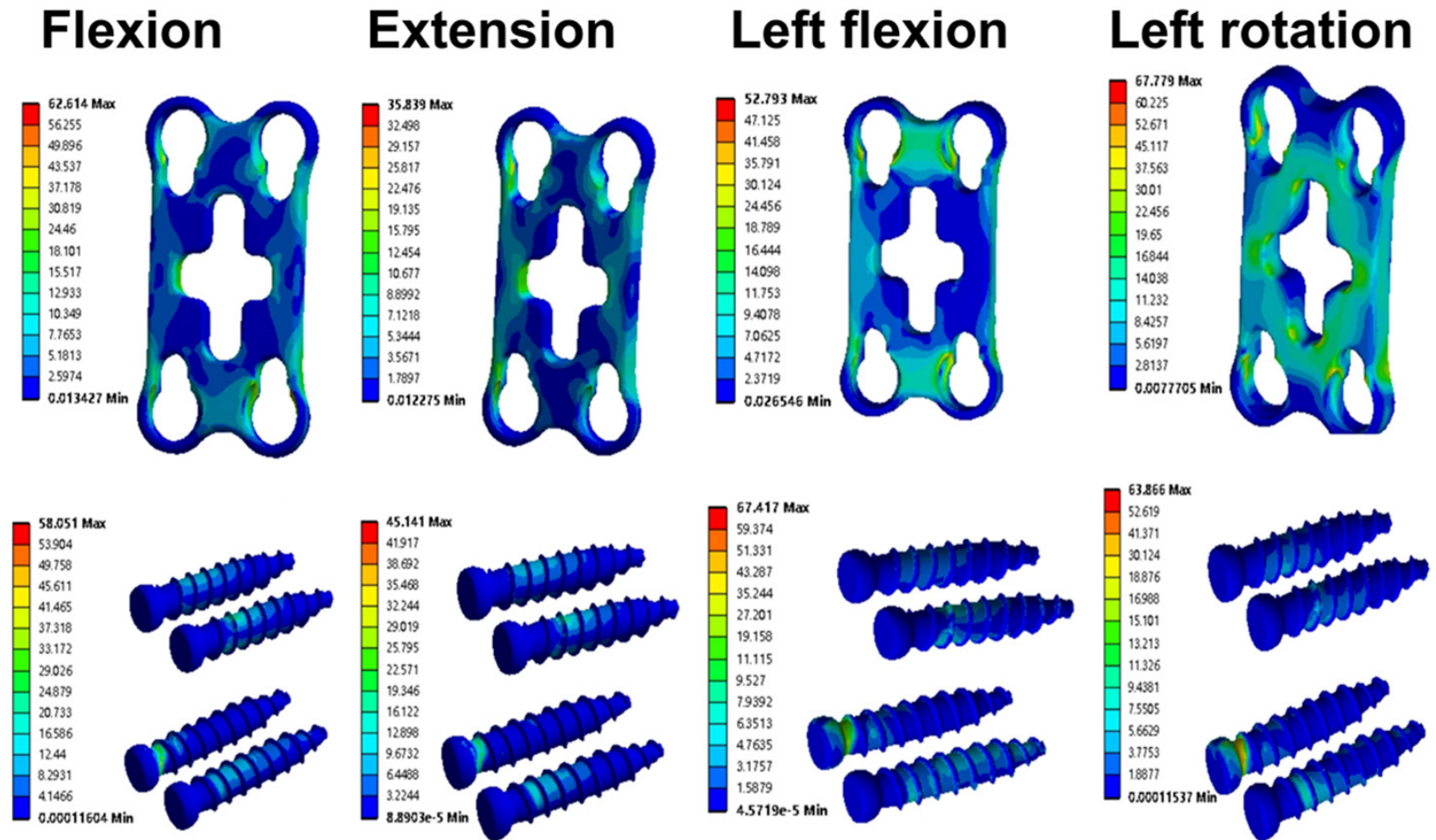


Figure 13. The stress cloud diagram of the front titanium plate and screws of the type 6 of lateral mass injury.

was little difference in ROM between the stability of complete and partial split fractures, and a large difference between the severe and mild avulsion fractures. Further analysis of different locomotion postures also found greater locomotion in AF and LF. This suggests that the lateral mass injury mainly affects the stability of ipsilateral flexion motion.

### *Stress distribution*

Unilateral facet joint fracture and dislocation of the subaxial cervical spine are usually caused by a distractive flexion injury. Wang et al. [21] first established a model of simple anterior fixation for different segments of distractive flexion injury using the three-dimensional FE analysis technique. Further mechanical analysis confirmed that distractive flexion injuries involved C6-7 and C7-T1, and the stress to the screw and plate after simple anterior fixation was higher than that to the cranial segments, suggesting that a combined anterior and posterior approach should be performed. Possible reasons for this phenomenon are as follows: ① the cervical thoracic segment, especially the C7-T1 segment, is difficult to reveal during the operation, and the shoulders may affect imaging during the operation. During the operation, some patients with unsatisfactory reduction may be missed, leading to internal fixation. ② the appearance of failure may occur because the cervical thoracic junction is located where the physiological lordosis of the cervical spine and the physiological kyphosis of the thoracic spine meet, and the existence of the T1 slope places stress on intervertebral implants. However, from the perspective of the incidence of SCFDs, a review by Aebi et al. [22] in 2010 pointed out that C5-6 and C6-7 accounted for approximately 55% of all injuries, and the incidence of C7-T1 was the lowest, at only 4.3%. Therefore, the conclusions of this study cannot guide the clinical decision-making of most patients. In addition, due to the differences in the intensity and direction of violence among different patients, there are also differences in the injury patterns of bone and ligament, which were not included in previous studies. In this study, we first confirmed that different damage morphologies of the lateral mass can affect titanium plate and screw stress. Plate and screw stress of type 4 was higher than that of the remaining five types. The stress of plates and screws of the same type with different types of lateral mass damage was further compared. The stress in type 1

was higher than that in type 2, and that in type 3 was higher than that in type 5. Further analysis of the stress of plate and screw in different motion positions showed that the stress was greater in AF and LF. This also suggests that lateral mass damage may lead to loss of ipsilateral stability and increase the stress of anterior implant. Therefore, the more severe the damage of the lateral mass, the greater the concentration of the mechanical stress on the plate and screw. These findings also support our previous findings that the posterior ligament-bone injury classification and severity (PLICS) score quantifies the severity of ligament-bone injury to the posterior three pillars of the subaxial cervical spine [6, 7]. There is a certain biomechanical basis for assigning the severity of lateral mass damage based on different damage morphology. When a PLICS score of  $\geq 7$  was accompanied by type 4 lateral mass injury, the risk of postoperative failure after an anterior-only reconstruction was high and supplemental posterior strengthening can be considered.

This study has some limitations. First the data was from a healthy adult volunteer, which limited the statistical analysis. More samples with follow-up may draw a more complete conclusion. Second, although muscle is the initiating factor and is an important stress conduction structure for subaxial cervical motion, only bones, ligaments, and intervertebral discs were included in the model, because there are a large number of muscles in the lower cervical segment, with complex shapes of macro and micro muscle fibers. Additionally, it is difficult to achieve personalized reproduction using FE technology due to different degrees of cervical muscle injury that may occur. Third, the model is relatively simple, and the material assignment of the model is relatively uniform. However, bone, intervertebral disc, and ligament materials are composites, which are not uniformly distributed and are anisotropic. Therefore, some differences between the model predictions and reality exist. Clinically, the shapes of lateral mass injuries are complex, a further clarification of the influence of the use of a single variable to assess the stability of internal fixation is needed.

### **Conclusion**

A three-dimensional FE modeling analysis method was used to compare left lateral mass biomechanical stability after being subjected to

different degrees of split, avulsion, and burst damage states. The more severe the injury, the higher the stress on the plate and screw with an exercise load. The type 4 lateral mass injury, characterized with ipsilateral pedicle and lamina junction fractures, significantly affected the biomechanical stability after simple anterior fixation.

### Acknowledgements

The medical ethics committee of the Honghui Hospital of Xi'an Jiaotong University approved the study (No. 202102007) in accordance with the relevant guidelines and regulations. Informed consent was obtained from the patient.

We thank national natural science foundation of China (No. 81830077 for Dingjun Hao) for providing the grant.

### Disclosure of conflict of interest

None.

**Address correspondence to:** Dingjun Hao, Department of Spine Surgery, Honghui Hospital, Xi'an Jiaotong University, No. 76, Nanguo Road, District of Beilin, Xi'an 710054, Shaanxi, China. Tel: +86-18792883498; E-mail: dingjun.hao@qq.com

### References

- [1] Vaccaro AR, Hulbert RJ, Patel AA, Fisher C, Dvorak M, Lehman RA Jr, Anderson P, Harrop J, Oner FC, Arnold P, Fehlings M, Hedlund R, Madrazo I, Rehtine G, Aarabi B and Shainline M. The subaxial cervical spine injury classification system: a novel approach to recognize the importance of morphology, neurology, and integrity of the disco-ligamentous complex. *Spine (Phila Pa 1976)* 2007; 32: 2365-2374.
- [2] Gao W, Wang B, Hao D, Zhu Z, Guo H, Li H and Kong L. Surgical treatment of lower cervical fracture-dislocation with spinal cord injuries by anterior approach: 5- to 15-year follow-up. *World Neurosurg* 2018; 115: e137-e145.
- [3] Vaccaro AR, Schroeder GD, Kepler CK, Cumhur Oner F, Vialle LR, Kandziora F, Koerner JD, Kurd MF, Reinhold M, Schnake KJ, Chapman J, Aarabi B, Fehlings MG and Dvorak MF. The surgical algorithm for the AOSpine thoracolumbar spine injury classification system. *Eur Spine J* 2016; 25: 1087-1094.
- [4] Liu K and Zhang Z. A novel anterior-only surgical approach for reduction and fixation of cervical facet dislocation. *World Neurosurg* 2019; 128: e362-e369.
- [5] Liu K and Zhang Z. Comparison of a novel anterior-only approach and the conventional posterior-anterior approach for cervical facet dislocation: a retrospective study. *Eur Spine J* 2019; 28: 2380-2389.
- [6] Yang JS, Liu P, Liu TJ, Zhang HP, Zhang ZP, Yan L, Zhao QP, He BR, Tuo Y, Zhao YT, Huang DG and Hao DJ. Posterior ligament-bone injury classification and severity score: a novel approach to predict the failure of anterior-only surgery for subaxial cervical facet dislocations. *Spine (Phila Pa 1976)* 2021; 46: 209-215.
- [7] Yang JS, Liu P, Liu TJ, Zhang HP, Zhang ZP, Yan L, Tuo Y, Chen H, Zou P, Li QD, Zhao YT and Hao DJ. When is the circumferential stabilization necessary for subaxial cervical fracture dislocations? The posterior ligament-bone injury classification and severity score: a novel treatment algorithm. *Eur Spine J* 2021; 30: 524-533.
- [8] Feng G, Hong Y, Li L, Liu H, Pei F, Song Y, Huang F, Tu C, Li T, Gong Q, Liu L, Zeng J, Kong Q and Gupte M. Anterior decompression and non-structural bone grafting and posterior fixation for cervical facet dislocation with traumatic disc herniation. *Spine (Phila Pa 1976)* 2012; 37: 2082-2088.
- [9] DePasse JM, Durand W, Eltorai AEM, Palumbo MA and Daniels AH. Timing of complications following posterior cervical fusion. *J Orthop* 2018; 15: 522-526.
- [10] Yee TJ, Swong K and Park P. Complications of anterior cervical spine surgery: a systematic review of the literature. *J Spine Surg* 2020; 6: 302-322.
- [11] Zhang X, Gao Y, Gao K, Yu Z, Lv D, Ma H and Zhai G. Factors associated with postoperative axial symptom after expansive open-door laminoplasty: retrospective study using multivariable analysis. *Eur Spine J* 2020; 29: 2838-2844.
- [12] Theodotou CB, Ghobrial GM, Middleton AL, Wang MY and Levi AD. Anterior reduction and fusion of cervical facet dislocations. *Neurosurgery* 2019; 84: 388-395.
- [13] Woodworth RS, Molinari WJ, Brandenstein D, Gruhn W and Molinari RW. Anterior cervical discectomy and fusion with structural allograft and plates for the treatment of unstable posterior cervical spine injuries. *J Neurosurg Spine* 2009; 10: 93-101.
- [14] Razack N, Green BA and Levi AD. The management of traumatic cervical bilateral facet fracture-dislocations with unicortical anterior plates. *J Spinal Disord* 2000; 13: 374-381.
- [15] Sribnick EA, Hoh DJ and Dhall SS. Traumatic high-grade cervical dislocation: treatment strategies and outcomes. *World Neurosurg* 2014; 82: 1374-1379.

## Biomechanical study of LM injury in SCFDs

- [16] Panjabi MM, Brand RA Jr and White AA 3rd. Mechanical properties of the human thoracic spine as shown by three-dimensional load-displacement curves. *J Bone Joint Surg Am* 1976; 58: 642-652.
- [17] Ng HW, Teo EC, Lee KK and Qiu TX. Finite element analysis of cervical spinal instability under physiologic loading. *J Spinal Disord Tech* 2003; 16: 55-65.
- [18] Panjabi MM, Cholewicki J, Nibu K, Babat LB and Dvorak J. Simulation of whiplash trauma using whole cervical spine specimens. *Spine (Phila Pa 1976)* 1998; 23: 17-24.
- [19] Eck JC, Humphreys SC, Lim TH, Jeong ST, Kim JG, Hodges SD and An HS. Biomechanical study on the effect of cervical spine fusion on adjacent-level intradiscal pressure and segmental motion. *Spine (Phila Pa 1976)* 2002; 27: 2431-2434.
- [20] Chang UK, Kim DH, Lee MC, Willenberg R, Kim SH and Lim J. Range of motion change after cervical arthroplasty with ProDisc-C and prestige artificial discs compared with anterior cervical discectomy and fusion. *J Neurosurg Spine* 2007; 7: 40-46.
- [21] Wang Z, Zhao H, Liu JM, Chao R, Chen TB, Tan LW, Zhu F, Zhao JH and Liu P. Biomechanics of anterior plating failure in treating distractive flexion injury in the caudal subaxial cervical spine. *Clin Biomech (Bristol, Avon)* 2017; 50: 130-138.
- [22] Aebi M. Surgical treatment of upper, middle and lower cervical injuries and non-unions by anterior procedures. *Eur Spine J* 2010; 19 Suppl 1: S33-39.